Electrically Conductive Adhesive with π-Conjugated Self-Assembled Molecular Wire Junctions for Enhanced Electrical and Thermal Properties

Rongwei Zhang, Yi Li, Myung Jin Yim, Kyoung Sik Moon, *Daoqiang Daniel Lu, and C. P. Wong
School of Materials Science and Engineering, Georgia Institute of Technology
771 Ferst Drive, Atlanta, GA, 30332, USA
* Intel Corporation, 5000 W. Chandler Blvd, Chandler, AZ 85226
Email: cp.wong@mse.gatech.edu Phone: 404-894-2846 Fax: 404-894-9140

Abstract

Anisotropic conductive adhesives/films (ACAs/ACFs) have been developed as a promising lead-free interconnect material in the electronic industry. However, due to the restricted contact area and poor interfacial bonding between ACAs and metal bond pads, the ACA joints have lower electrical conductivity and poorer current carrying capability than that of solders. In this study, we investigated the current carrying capability of submicron-sized (~500 nm) silver (Ag) particles in ACA. It was found that the submicron-sized Ag particles have higher current carrying capability (~3400 mA) than micro-sized Au-coated polymer particles (~2000 mA) and Ag nanoparticles (~2500 mA). More importantly, with the introduction of self-assembled monolayer (SAM) on a Ag particle surface, the electrical conductivity and current carrying capability of the ACAs could be significantly improved. By studying the adsorption behavior and thermal stability of the SAMs on submicron-sized Ag particles with ATR FT-IR, Raman spectroscopy and TGA, the crucial factors that govern the improved electrical properties were discussed.

Introduction

Tin-lead solder alloy has been widely used in the electronic industry. However, there are some intrinsic problems associated with tin-lead solder, such as environmental concerns and relatively high processing temperature limiting their future applications. Considerable advances have been made in the development of lead-free solders and electrically conductive adhesives (ECAs) as promising alternatives. Due to their higher melting point than that of eutectic tin/lead solder, lead-free alloys cause some problems such as higher stress generated in a package, requirement of more expensive substrates, and more serious package pop-corning problem when the package is assembled on the printed wiring board (PWB). On the other hand, ECAs have the advantages of environmental friendliness, mild processing conditions, fewer processing steps, lower stress on the substrates, and finer pitch interconnect capability.

There are two types of conductive adhesives: anisotropic conductive adhesives/films (ACAs/ACFs) and isotropic conductive adhesives (ICAs). ICAs are electrically conductive along all the directions and the loading level of conductive fillers (mostly Ag flakes) exceeds the percolation threshold, while ACAs/ACFs provide unidirectional electrical conductivity in the vertical or *z*-axis by using a relatively low filler loading of conductive fillers. The loading level of ACA is far below the percolation threshold and the low loading is insufficient for interparticle contact, which prevents conductivity in the *x–y* plane of the adhesives. A cross-section of a joint formed by an ACA between the IC/substrate is shown in Figure 1. The numerous advantages of ECAs over the conventional solder technology allow the wide applications of ECAs in the fields of liquid crystal display (LCD) and smart cards where low temperature interconnects are needed. Nevertheless, some challenging problems have to be solved before the replacement of tin-lead solder with ECAs such as lower electrical conductivity, conductivity fatigue in reliability testing, limiting current-carrying capability, and poor impact strength [1, 2].

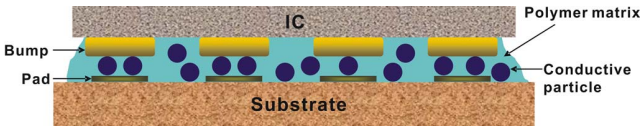

Figure 1 A cross-section of an ACA junction.

Over the past two decades, self-assembled monolayers (SAMs) have attracted significant interests due to their potential applications in corrosion prevention, lubrication, wetting control, wear prevention, oxidation retardation, adhesion and molecular electronic devices [3]. In particular, high electron transport in metal-SAM molecule(s)-metal junctions has enabled the applications of SAMs in molecular electronics. Significant decrease (2 orders of magnitude) in metal-molecule contact resistance can be achieved by using alkanethiol-based SAM junction. This is due to chemically bonded SAM-metal pad contacts instead of nonbonded (mechanical) contacts [4]. Generally, the Fermi level of the noble metal electrodes lies within the highest occupied molecular orbital (HOMO)-lowest unoccupied molecular orbital (LUMO) gap of contact molecules. By tuning the work function of the electrodes with SAMs, tunneling resistance could be significantly reduced and thus improvement of electrical conduction can be obtained. Furthermore, the efficiency of charge transport through π-conjugated molecules sandwiched between two electrodes further contributes to the enhanced electrical conduction of metal-molecule contacts. Besides the improvement of electrical conduction, Kobayashi et al. demonstrated the ability of SAMs to control the charge-carrier density in organic field-effect transistors (FETs) [5].

Taking advantages of those unique properties of SAMs, our research group has introduced π-conjugated self-assembled molecular wire junctions to improve the electrical properties of anisotropic conductive adhesives (ACAs) [6]

and nonconductive films (NCFs) [7] for the electronic interconnects in previous work [8]. The resulting ACAs and NCFs exhibited improved electrical conduction, higher current carrying capability and better thermal stability of SAM-treated joint. Crucial for successful applications of SAMs in ACAs and NCFs are interfacial properties (chemisorption or physisorption), the characteristics of the molecules (conjugated or unconjugated, thermal stability, etc), surface binding geometry, and packing density. Therefore, current work will investigate the effects of those factors on the performance of ACAs in detail by using a series of molecules with different functional groups and structures, providing an insight into the factors that govern enhanced electrical properties of resulting ACAs. Furthermore, thermal stability can be further improved by selecting the molecules for SAMs that have high affinity to the substrate and achieve higher reliability. The resulting ACAs with better electrical conduction, higher current-carrying capability, enhanced thermal stability and good reliability will enable their applications in fine pitch and high performance interconnects in microelectronics.

Experimental

Two types of SAMs (SAM1 and SAM2) with different functional groups were used. Submicron-sized Ag particles (~500 nm) were treated in the SAM solutions and then sonicated for 10 min. After the SAM treatment for 24 hrs, the samples were removed from the solution and rinsed with solvent used for the dissolution of the molecules in order to remove excess un-adhered SAM molecules. Ag particles were separated from SAM solutions by centrifuge and then dried under vacuum before the characterization. The coating of SAM on Ag particles was characterized by Attenuated Total Reflectance Infrared Fourier Transform spectroscopy (ATR FT-IR) and Raman spectroscopy. Raman spectra were obtained using Bruker Optics FT-Raman (Equinox 55) with near infrared (NIR) lasers (λ=1064 nm). In a typical measurement, the laser power at the sample position was 300-500 mW and the resolution is 2 cm^{-1}.

Weight loss of untreated and SAM-treated Ag particles during heating was monitored using a thermogravimetric analyzer (TGA) from TA Instruments, model 2050. The temperature was raised from 25 °C to 500 °C at a heating rate of 10 °C/minute in a nitrogen atmosphere. To obtain the thermal behavior of SAM on Ag particles, the sample were heated at 150 °C and 200 °C for 0.5 hr and then characterized by Raman spectroscopy.

For characterizing the electrical properties of submicron-sized Ag particle filled ACA, Ag particles were added in a polymeric resins, in which bisphenol-F type epoxy, anhydride and imidazole were used as epoxy, hardener and catalyst, respectively. The electrical contact resistance of the ACA joints (contact area: 150×150 μm^2) was measured by a four-point probe method [6]. The applied four point probe currents were varied by a power supplier (HP model 6553A, HP Hewlett Packard, Palo Alto, CA) and the voltage of the interconnect joints were measured by a Keithley 2000 multimeter (Cleveland, Ohio).

Results and Discussion

Study of the Interaction between SAMs and Submicron-sized Ag Particles

Figure 2 shows the ATR FT-IR spectra of Ag, SAM1-coated Ag and SAM2-coated Ag. Compared with the spectrum of Ag, SAM-coated Ag shows the obvious adsorption in the range of 2800-3000 cm^{-1} due to the stretching of C-H of SAM molecules, indicating that Ag has been coated with SAM1 and SAM2. Moreover, the disappearance of absorption of –COOH at 1700 cm^{-1} and appearance of two peak at 1500 cm^{-1} ($\nu_a(COO^-)$) and 1420 cm^{-1} ($\nu_s(COO^-)$) suggest that carboxylic acid may have been converted to carboxylate after our modification. However, it seems that ATR FT-IR is not sensitive to detect the configuration of the absorbed SAMs. Surface-enhanced Raman spectroscopy (SERS) is a very useful surface spectroscopic technique for the study of the orientation of various kinds of molecules adsorbed on noble metal surfaces (Au, Ag and Cu) due to its high spectral resolution and the spectral sensitivity from monolayer adsorbates on those metal surfaces. Raman spectra of SAM, Ag, SAM-treated Ag at room temperature, baked at 150 °C and 200 °C for 0.5 hr are shown in Figure 3 (SAM1) and Figure 4 (SAM2). The assignment of peaks is based on the references [9-12] and summarized in Table 1.

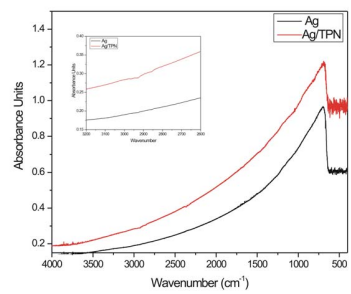

(a)

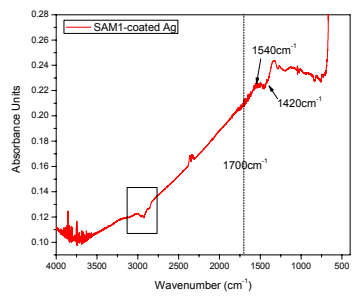

(b)

Figure 2 (a) ATR FT-IR spectra of Ag, SAM2-coated Ag and (b) SAM1-coated Ag.

In Figure 3, the C=O stretching peak at 1629 cm^{-1} of SAM1 disappeared in the spectrum of SAM1 absorbed on the Ag surface. Instead, the symmetric stretching and

Table 1 Spectral data and the vibrational assignments of SAM1 and SAM2.

SAM1			SAM2		
Ordinary Raman (ν/cm^{-1})	μ-Ag SERS (ν/cm^{-1})	Assignment	Ordinary Raman (ν/cm^{-1})	μ-Ag SERS (ν/cm^{-1})	Assignment
631		6b	517		δ_{as}(CN)
670		4	559		γ_{as}(CN)
	703	δ(COO$^-$)	655		6b
830	858	1	813		1
1123	1129	7a	1173		7a
1283		ν(C-O)		1194	13
	1405	ν_s(COO$^-$)	1608	1604	8a
1448		δ(OH)	2236	2234	ν(CN)
1610	1606	8a	3071		ν_s(CH)
1629		C=O stretching	3080		ν_{as}(CH)
3075		ν_s(C-H)			
3087		ν_{as}(C-H)			

bending modes of COO$^-$ appear at 1405 and 703 cm^{-1}. Hence, SAM1 was chemisorbed on the silver surface via two Ag-COO$^-$ bonds after deprotonation and lies flat on the Ag particle surface. Moreover, according to the electromagnetic enhancement mechanism for SERS, the absence of the peak at 3086 cm^{-1} due to the C-H stretching further indicate that SAM1 lies flat on the Ag surface [13-15].

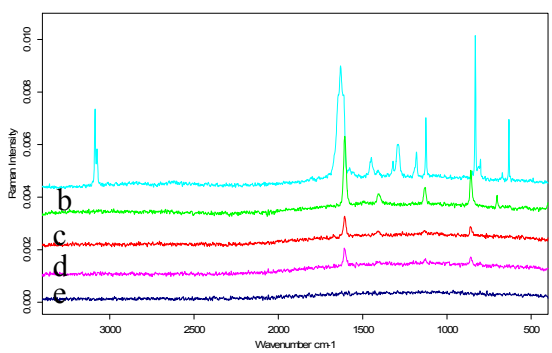

Figure 3 Raman spectra of (a) SAM1, (b) SAM1 adsorbed on Ag particles, SAM1 adsorbed on Ag particles baked at (c) 150 °C and (d) 200 °C for 0.5 hr respectively, and (e) Ag particles.

Aromatic nitriles can coordinate with Ag by three different ways, namely the nitrogen lone-pairs, the C≡N π system and the π system of the benzene ring. Generally, a majority of aromatic nitriles were absorbed on the silver surface via C≡N π system rather than the nitrogen lone-pair electrons. A slight increase in C≡N stretching frequency of SAM2 was attributed to the disruption of conjugation, as was observed when SAM2 adsorbed on the silver sol (silver colloidal particle) surface. However, upon surface adsorption of SAM2 on a submicron-sized Ag particle, C≡N stretching frequency decreases. C≡N stretching frequency can either decease or increase depending on the relative importance of nitrile-to-metal π donation and conjugation. More importantly, substantial broadening of C≡N stretching strongly indicates that C≡N of the adsorbed SAM2 interacts directly with Ag particle. The complete absence of C-H stretching band in the SERS spectra of SAM2 implies that the benzene ring of SAM2 lies flat on the Ag particle surface.

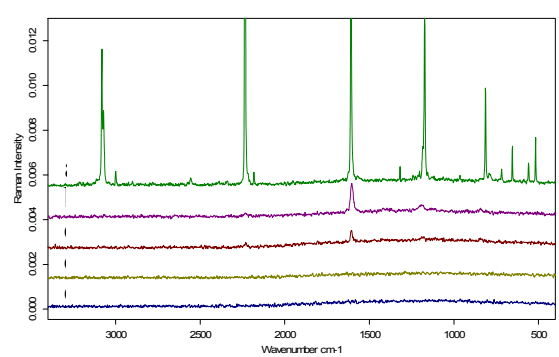

Figure 4 Raman spectra of (a) SAM2, (b) SAM2 adsorbed on Ag particles, SAM2 adsorbed on Ag particles baked at (c) 150 °C and (d) 200 °C for 0.5 hr respectively, and (e) Ag particles.

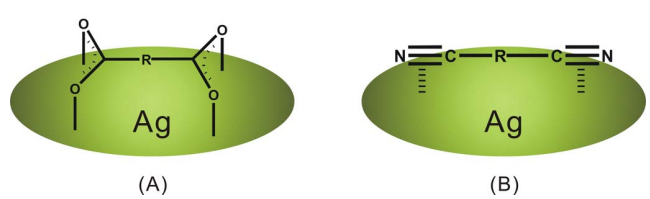

Figure 5 Alignments of SAM1 and SAM2 on a submicron-sized Ag particle surface.

Thermal Stability

Thermal stability of SAM molecules on Ag particles is of great importance for their applications in ACA since the SAM coating should be survived during ACA bonding or at reflow temperature. The thermal stability of SAM molecules was evaluated by SERS and TGA. The SERS in Figure 3 indicates that SAM1 was partially detached from the Ag surface after baking at 150 °C for 0.5 hr and no further detachment was observed at 200 °C for 0.5 hr. For SAM2, it was partially detached from the Ag surface at 150 °C for 0.5 hr and almost completely removed from the surface at 200 °C for 0.5 hr (see Figure 4).

To characterize the SAM on Ag particle surface, the weight change of Ag particles was measured by TGA in air and N_2 and the results are shown in Figure 6. More weight was gained for Ag particles in air than in N_2 at ca. 190 °C, which may due to the oxidation of Ag particles and then the formed Ag oxides decompose into metallic Ag. Waterhouse et al. reported that the transformation of AgO to Ag_2O occurred with heating in the 100-200 °C region and further thermal decomposition of Ag_2O to Ag at the temperature higher than 350 °C [17]. Kolobov et al. reported that the complete decomposition of AgO to metallic Ag at considerably lower temperature than reported earlier, namely, 160 °C [18]. Zhang et al. reported AgO can be partially decomposed at 190 °C characterized by X-ray diffraction (XRD) [19]. The thermal decomposition of Ag oxides may highly depend on preparation methods and their processing history. Moreover, the second run of TGA indicates there is no obvious weight gain, which means Ag did not oxidize in the air under the experimental condition. Therefore, we concluded that there may have some silver oxide on Ag particle surface. The possible mechanism is shown below:

(1)Oxidation of Ag_2O at 150-190 °C

$$Ag_2O\,(s) + 1/2O_2\,(g) \xrightarrow{\Delta} Ag_2O_2\,(s)$$

(2) Decomposition of Ag oxides at 190-250 °C

$$Ag_2O_2\,(s) \xrightarrow{\Delta} Ag_2O\,(s) + 1/2O_2\,(g)$$

$$Ag_2O\,(s) \xrightarrow{\Delta} 2Ag\,(s) + 1/2O_2\,(g)$$

After treatment with SAM1 or SAM2, no obvious weight gain was observed in the range of 190 to 250 °C. The possible reasons: (1) monolayer of SAM1 or SAM2 on Ag particle surface may prevent/retard the oxidation of Ag_2O; (2) Reaction of Ag_2O with acids:

$$R\text{-}COOH + Ag_2O \longrightarrow R\text{-}COOAg + H_2O$$

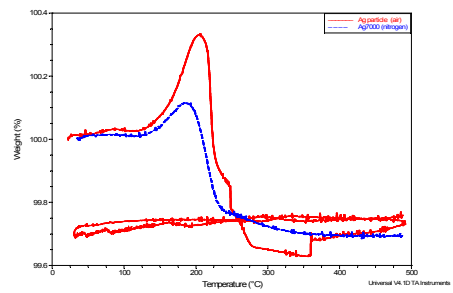

Figure 6 Thermogravimetric analyses of Ag particles in air and N_2.

TGA measurements of SAM-treated Ag particles are shown in Figure 7 and around 0.4% weight loss were observed. The weight loss may correspond to the decomposition of the SAM molecules and the transformation of silver oxides to metallic Ag, which suggests the SAM organic compounds have been well coated on the Ag particles due to the interaction between Ag particles and carboxylic acid/nitrile functional groups. TGA results are in well consistency with ATR FT-IR and SERS.

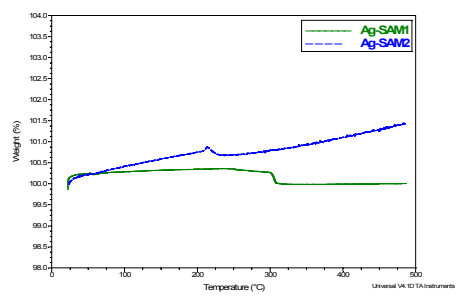

Figure 7 Thermogravimetric analyses of Ag particles treated with SAM1 and SAM2 for 24 hrs.

Electrical Properties

The current-voltage (I-V) curve of submicron-sized Ag filled ACAs is shown in Figure 8 (a). Compared with control sample (ACA with unmodified Ag particles), ACAs with SAM1-treated Ag particles exhibited decreased resistance while the ACA with SAM2-treated Ag particles showed higher resistance. Previous researches in our group have demonstrated that SAM molecular wires can act as electrical junctions between the conductive filler of the ACA and the contact pad of the substrate. As such, the electrical path at the interface could be enhanced, which enables the improved conductivity. For SAM2, the weak interaction of Ag with the molecule and flat surface alignment may weaken the interaction between Ag particle and metal bond pads, resulting in decreased conductivity. Compared with SAM2, SAM1 has stronger affinity to Ag particles and more importantly, the removal of silver oxide on the Ag surface may play a key role in the increased conductivity. As a result, the conductivity increases, although it lies flat on the particle surface. For ACA filled with SAM1-treated Ag, the resistance decreased (see Figure 8 (b)). Moreover, the submicron-sized

Ag particles have higher current carrying capability (~3400 mA) than micro-sized Au-coated polymer particles (~2000 mA) and Ag nanoparticles (~2500 mA) [20]. More importantly, with the introduction of self-assembled monolayer (SAM) on a Ag particle surface, the current carrying capability increased steadily from 3400 mA for control sample without SAM-treatment to about 4000 mA with SAM-treated samples.

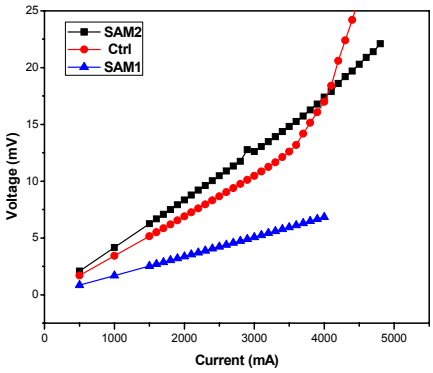

(a)

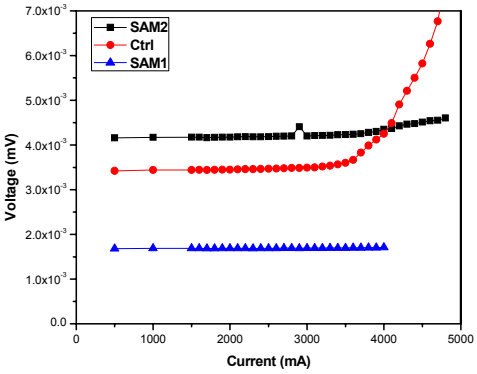

(b)

Figure 8 (a) I-V curve of ACA filled with Ag particles (Ctrl), SAM1-treated Ag particles and SAM2-treated Ag particles; (b) Corresponding I-R curves.

Conclusions

Surface alignment of SAM molecules and their thermal stability on submicron-sized Ag particles have been investigated by ATR FT-IR, Raman spectroscopy and TGA. With the introduction of SAM-treated Ag particles, the electrical conductivity and current carrying capability of ACAs could be significantly improved. The crucial factors that govern enhanced electrical properties of the resulting ACAs interconnect have been explored based on the study on the characteristics of SAM molecules, interaction between Ag particles and SAM molecules, molecular chain orientation of SAM molecules on Ag particle surface and their thermal stability. With the improved electrical conductivity and current carrying capability, ACA will be expected to have a promising application for high electrical performance and solder replacement in fine pitch interconnect.

Acknowledgments

The authors would like to thank Intel Corporation for the financial support. The authors would also like to thank Dr Robert Braga and Dr Boris Mizaikoff in the School of Chemistry and Biochemistry at Georgia Institute of Technology for valuable discussion of Raman spectrometry.

References

[1] Y. Li and C. P. Wong, "Recent advances of conductive adhesives as a lead-free alternative in electronic packaging: materials, processing, reliability and applications," *Materials Science & Engineering, R: Reports,* vol. R51 (2006), pp. 1-35.

[2] Y. Li, K.-s. Moon, and C. P. Wong, "Electronics without lead," *Science (Washington, DC, United States),* vol. 308 (2005), pp. 1419-1420.

[3] J. C. Love, L. A. Estroff, J. K. Kriebel, R. G. Nuzzo, and G. M. Whitesides, "Self-Assembled Monolayers of Thiolates on Metals as a Form of Nanotechnology," *Chemical Reviews (Washington, DC, United States),* vol. 105 (2005), pp. 1103-1169.

[4] X. D. Cui, X. Zarate, J. Tomfohr, O. F. Sankey, A. Primak, A. L. Moore, T. A. Moore, D. Gust, G. Harris, and S. M. Lindsay, "Making electrical contacts to molecular monolayers," *Nanotechnology,* vol. 13 (2002), pp. 5-14.

[5] S. Kobayashi, T. Nishikawa, T. Takenobu, S. Mori, T. Shimoda, T. Mitani, H. Shimotani, N. Yoshimoto, S. Ogawa, and Y. Iwasa, "Control of carrier density by self-assembled monolayers in organic field-effect transistors," *Nature Materials,* vol. 3 (2004), pp. 317-322.

[6] Y. Li, K.-S. Moon, and C. P. Wong, "Adherence of self-assembled monolayers on gold and their effects for high-performance anisotropic conductive adhesives," *Journal of Electronic Materials,* vol. 34 (2005), pp. 266-271.

[7] Y. Li, M. J. Yim, and C. P. Wong, "High performance nonconductive film with p-conjugated self-assembled molecular wires for fine pitch interconnect applications," *Journal of Electronic Materials,* vol. 36 (2007), pp. 549-554.

[8] Y. Li, M. J. Yim, and C. P. Wong, "Introduction of self assembled monolayer molecular wires in electronic packaging interconnects for enhanced electrical properties, fine pitch capability and reliability," *U.S. Patent pending GTRC Invention No. 3975,* (2006).

[9] F. J. Boerio and P. G. Roth, "Vibrational analysis of terephthalate and terephthalate-d4 ions," *Applied Spectroscopy,* vol. 41 (1987), pp. 463-7.

[10] M. W. Lee, M. S. Kim, and K. Kim, "Infrared and Raman spectroscopic study of terephthalic acid

adsorbed on silver surfaces," *Journal of Molecular Structure,* vol. 415 (1997), pp. 93-100.

[11] H. S. Kim, S. J. Lee, N. H. Kim, J. K. Yoon, H. K. Park, and K. Kim, "Adsorption Characteristics of 1,4-Phenylene Diisocyanide on Gold Nanoparticles: Infrared and Raman Spectroscopy Study," *Langmuir,* vol. 19 (2003), pp. 6701-6710.

[12] S. H. Cho, Y. J. Lee, M. S. Kim, and K. Kim, "Infrared and Raman spectroscopic study of 1,2-benzenedithiol adsorbed on silver," *Vibrational Spectroscopy,* vol. 10 (1996), pp. 261-70.

[13] C.-R. Lee, S. J. Bae, M.-S. Gong, K. Kim, and S.-W. Joo, "Surface-enhanced Raman scattering of 4,4'-dicyanobiphenyl on gold and silver nanoparticle surfaces," *Journal of Raman Spectroscopy,* vol. 33 (2002), pp. 429-433.

[14] A. Michota and J. Bukowska, "Surface-enhanced Raman scattering (SERS) of 4-mercaptobenzoic acid on silver and gold substrates," *Journal of Raman Spectroscopy,* vol. 34 (2003), pp. 21-25.

[15] K. H. Yu, J. M. Rhee, S. Ko, and S.-C. Yu, "Surface-enhanced raman scattering study of 4-biphenylcarboxylic acid and a liquid crystalline oligomer on different metal surfaces," *Langmuir,* vol. 17 (2001), pp. 8184-8187.

[16] S. H. Kim, S. J. Ahn, and K. Kim, "Vibrational Spectroscopic Study of 4-Cyanobenzoic Acid Adsorbed on Silver," *Journal of Physical Chemistry,* vol. 100 (1996), pp. 7174-80.

[17] G. I. N. Waterhouse, G. A. Bowmaker, and J. B. Metson, "The thermal decomposition of silver (I, III) oxide: A combined XRD, FT-IR and Raman spectroscopic study," *Physical Chemistry Chemical Physics,* vol. 3 (2001), pp. 3838-3845.

[18] A. V. Kolobov, A. Rogalev, F. Wilhelm, N. Jaouen, T. Shima, and J. Tominaga, "Thermal decomposition of a thin AgOx layer generating optical near-field," *Applied Physics Letters,* vol. 84 (2004), pp. 1641-1643.

[19] R. Zhang, D. Zhang, H. Mao, W. Song, G. Gao, and F. Liu, "Preparation and characterization of Ag/AgO nanoshells on carboxylated polystyrene latex particles," *Journal of Materials Research,* vol. 21 (2006), pp. 349-354.

[20] Y. Li and C. P. Wong, "High performance anisotropic conductive adhesives for lead-free interconnects," *Soldering & Surface Mount Technology,* vol. 18 (2006), pp. 33-39.